Investigation on the effect of warping on the stability behaviour of cold formed steel beam-columns

Sevugan J Rajkannu[1], Arul S Jayachandran[2]

Abstract
Design of cold formed steel beam-column members has always been a subject of research due to its complex behavior and its propensity for undergoing interactive buckling under axial loads and varying moments. This paper adds further dimension to the ongoing research on beam-columns by investigating the important aspects the 'warping' and 'bi-moment'. The experimental studies reported in literature on the effect of warping on beam-column behavior is very scarce. This may be due to the complex nature of experimental procedures to create free warping of the cross section under compression and bending. In this study the 'warping free' boundary condition is simulated using a specially designed loading fixture which transmit the load through the zero sectorial coordinate. Controlled experiments are conducted on cold formed steel lipped channel cross section beam-column members under both axial and eccentric compression. Companion numerical models for the experimental specimens are created using ABAQUS and calibration studies are carried out. The numerical study is extended to various loading situations for predicting the strength of members under different warping boundary conditions. The results of the present study show that for axial compression, the use of effective length factor of $K_t=0.5$ to account for warping restraint, lead to overestimation of the axial resistance of the CFS member as per AISI S100-2016. With the present experimental studies, it is seen that the use of warping restraint factor $K_t=0.8$ results in acceptably close predictions of beam-column capacities based on the linear interaction framework. The present paper also brings out the need for integrating the 'warping' in the beam-column non-linear interaction framework.

1. Introduction
Structural design of cold-formed steel (CFS) members are treated separately from hot-rolled steel design due to predominance of buckling effects. Structural design of CFS members are usually done using two methods 1) Effective Width Method (EWM) 2) Direct Strength method (DSM). The design of CFS members using EWM for complex cross sections is a very tedious process. The DSM, is already in vogue is based on elastic critical buckling load for various buckling modes obtained from a finite strip analysis. In DSM the failure of the CFS member is prescribed empirically taking into account interaction of local, distortional and global buckling and yielding failure. When DSM was proposed, the empirical equations have been developed based on available test data on local-global interaction behavior, available at that time and there has been continuous development thereafter.

[1] Research Scholar, Indian Institute of Technology Madras, India, <sevuganrajkannu@gmail.com>
[2] Professor, Indian Institute of Technology Madras, India, <aruls@iitm.ac.in>

Developments in DSM is not explained in this paper - readers may refer (Schafer, 2008) (Kumar and Kalyanraman 2014). The design resistances of CFS sections using DSM are prescribed based on some significant points on a signature curve (a plot of length versus buckling loads) buckling stress value calculated from a finite strip program CUFSM. The signature curve which is now being used is developed for members with simply supported flexural supports and warping free boundary condition at both ends. DSM neglects the effect of warping in strength of member. Warping deformation in the local and distortional buckling formulations was studied in (Adany and Schafer 2006), (Camotim et.al., 2010) using finite strip method and generalized beam theory respectively. The effect of warping in case of fixed boundary condition was investigated in (Gunalan and Mahendran 2013). (Piana et al., 2017) conducted series of experiment on cruciform section with warping free and warping restrained boundary conditions under axial compression. Traditionally, the effect of restrained warping is taken care by introducing an effective length factor for torsion as $K_t=0.5$ in the torsional buckling equation, resulting in enhanced buckling strength of the member. In construction practice, most members have warping restraint at their ends under axial compression thus the warping becomes an important design parameter.

The experimental data for members under axial compression with warping free boundary condition is very scarce in the literature. A series of tests on box-like section with small b/t ratio is shown in (Vlasov, 1964.), where no local buckling occurs before failure. The point loads were applied at zero sectorial coordinate of the channel section as shown in Fig. 1. To study the influence of warping restrained condition under pure compression (Moore and Currie 1988) conducted a series of tests on unlipped channel sections with warping free and warping restrained condition. The possibility to design of members dominated by warping torsion using DSM is given in (Bian, et al., 2016). The influence of bi-moments on thin walled Z section due to axial compressive load is presented in (Prokić, et al.,2015). The influence of warping in case of beam-column member will be higher due to the propensity for torsional deformation. The behaviour of members under combined loads was explained in (Chen and Atsuta 1976). Design of CFS beam-column is mainly based on the linear interaction (LI) equation in case of EWM and DSM. The axial strength (P_n), flexural strength (M_{nx}, M_{ny}) of the member calculated separately and applied in the linear interaction shown in Eq. (1).

$$\frac{P}{P_n} + \frac{C_{mx}M_x}{\alpha_x M_{nx}} + \frac{C_{my}M_y}{\alpha_y M_{ny}} \leq 1 \tag{1}$$

Where C_{mx}, C_{my} are the moment gradient factors, α_x, α_y are the moment amplification factor to account for second order effects.

$$C_{mx} = 0.6 - 0.4\frac{M_1}{M_2} \tag{2}$$

$$\alpha_x = \left(1 - \frac{P}{P_{ex}}\right) \tag{3}$$

Where M_1, M_2 are the end moments and P_{ex}, P_{ey} are the Euler buckling loads about the major and minor axes. Since many of CFS section are of mono symmetric open sections they fail in flexural-torsional buckling even in case of axial compression. The effect of eccentricity on the failure modes on mono-symmetric section is discussed in (Pekoz and Winter 1969). The experimental results from research reported in (Miller and Pekoz 1994), (Rasmussen, 2006),

(Rhodes.et.al 2000) show that the linear interaction equation for beam-column shown in Eq. (1) predicts member strength very conservatively. Linear interaction framework does not capture the actual behaviour and failure mode of the beam-columns. Effective width method (EWM) based on combined stress action was studied by (Kalyanaraman and Jayabalan 1994), using an iterative method. Test results of (Kalyanaraman and Rao 1998) matches with iterative procedure of combined action failed under local-global interaction buckling. DSM uses a software for calculation of the elastic buckling stress, it is easy to use the combined stress due to axial compression and bending instead of individual stress. A beam-column equation in nonlinear interaction (NLI) format, in terms of β, θ_{mm} and ϕ_{pm} is proposed by (Schafer, 2012). To validate the DSM formulation of nonlinear interaction 54 experiments (Torabian et.al., 2014) were conducted on the lipped channel section of 600S137-54 with uniform moment throughout the member. Application of nonlinear interaction to Z –section beam-column is reported in (Torabian et.al, 2015). The in-plane buckling behaviour of lipped channel section under beam-column action discussed in (Li et.al., 2016) shows that there is need for inclusion of the second order effects. The series of beam-column experiments on rack section (Vijayavengadesh Kumar and Arul Jayachandran 2016) shows the NLI is unconservative for linearly varying moment, also pointed out that the use of θ_{MM} and ϕ_{PM} corresponding to $M_{2y,min}$ and $M_{2y,max}$ values to be used in the nonlinear interaction format.
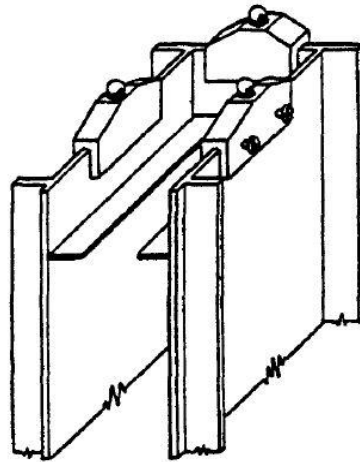
Figure 1: *Vlasov test setup for warping free
condition*

2. Warping – a parameter for design of CFS members
From the literature it is clearly known there are very few experimental studies are available on the effect of warping on the interactive buckling behavior of CFS members. The commonly used buckling formula for flexural torsion buckling (FTB) is based on the simply supported and warping free condition. According to authors' knowledge no experimental work is reported in the literature on beam-column behavior with warping free condition. In the present work, details of experiments conducted on warping free and warping restrained condition under axial and eccentric compression is reported. The results are compared with beam-column resistances calculated using AISI S100-2016.

3. Experimental investigation on effect of warping on member behavior

3.1 Selection of specimen

Based on an investigation using GBTUL and CUFSM, the size of lipped channel cross section is selected as 80x60x10 with 1.6 mm thick. Fig. 2 shows the elastic buckling curve for the selected lipped channel cross section under axial compression for various length. In CUFSM, signature curve is possible only for simply supported and warping free boundary condition whereas GBTUL has a provision to specify restrained warping boundary condition also. A member length of 1600 mm is chosen and from the analysis shows it is seen that the member is expected to buckle in flexural torsional buckling (FTB) under simply supported-warping free condition and distortional buckling under warping restrained condition.
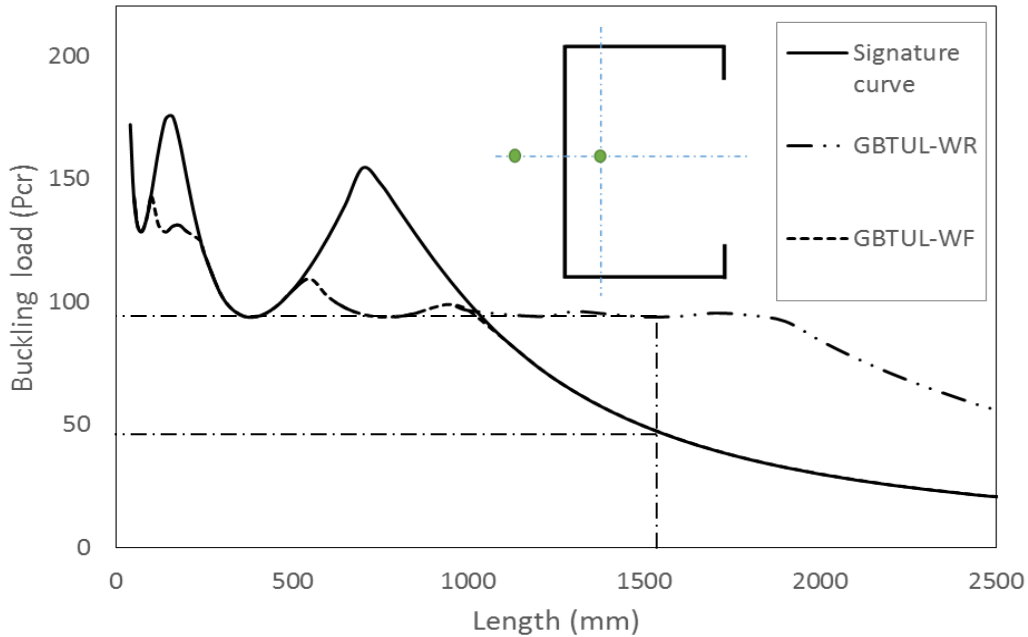
Figure 2: Elastic Buckling curve for lipped channel section under axial compression

3.2 Material property

Tensile coupon tests are made from the specimen form the web and flanges of lipped channel section. The tension coupon specimen is prepared based on the recommendation of ASTM A-370 and (Huang & Young, 2014). The coupon tests are carried in displacement controlled universal testing machine. The loading rate adopted for testing is 0.05 mm/minute up to yielding, and 0.8 mm/minute after yielding. The specimen is kept for relaxation for 5 minutes after yielding. Strain gauges are placed on both the side of the coupon. The average strain from the strain gauge is used for the calculation of Young's modulus. The material properties such as yield stress, ultimate stress and Young's modulus is summarized in Table 1. The average yield stress value is 238 MPa. Fig. 3 shows the plot of stress vs strain for the coupons. To study the effect of warping on lipped channel cross section, torsional parameters of section such as shear center and warping constant is found using the sectorial coordinate. The principal sectorial coordinate for the lipped channel cross section is given in Fig. 4b.

4

Table 1: Tension Coupon test results

Test	Yield Stress (MPa)	Ultimate Stress (Mpa)	Young's Modulus (GPa)
1	230	332	191.5
2	236	338	199.3
3	237	339	209.9
4	250	353	205.5
Mean	238.2	340.5	201.5
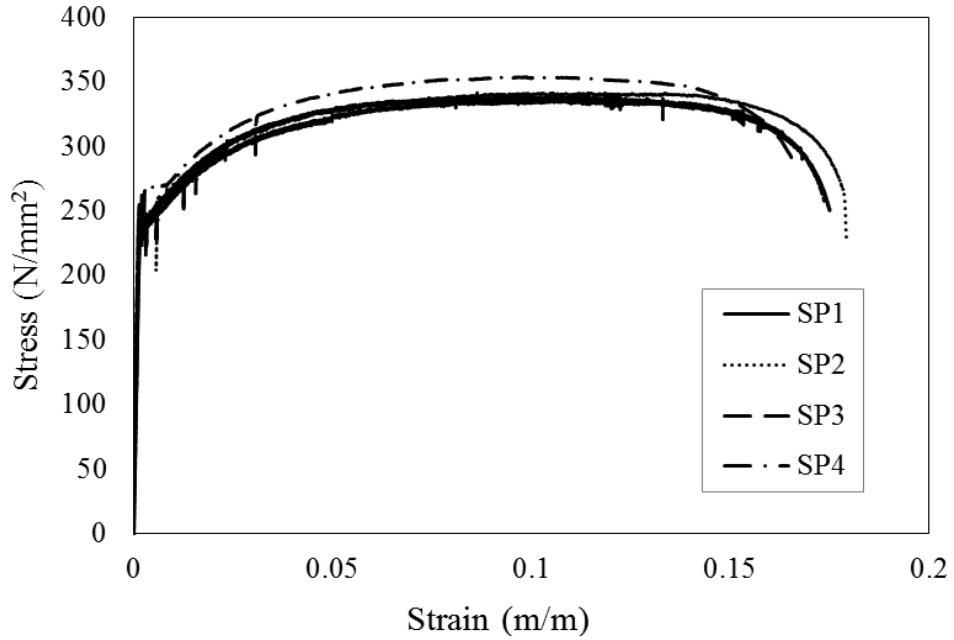
Figure 3: Tensile stress strain curve of the specimen
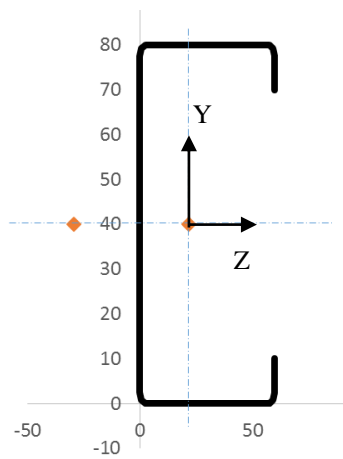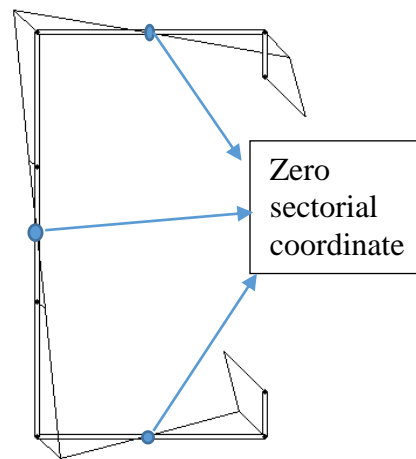
Figure 4: (a) cross section geometry (b) sectorial coordinate

3.3 Test set up to simulate free warping

In order to create free warping boundary condition under the compressive load, the load has to be applied at the point of zero sectorial coordinate such that the compressive load on the cross section does not create any external bi-moment. The end loading section should not restrain the out of plane deformation of cross section (warping) due to torsional deformation. To achieve the warping free boundary condition under compressive load, an end fixture was fabricated as shown in Fig. 5a.

a)   b)
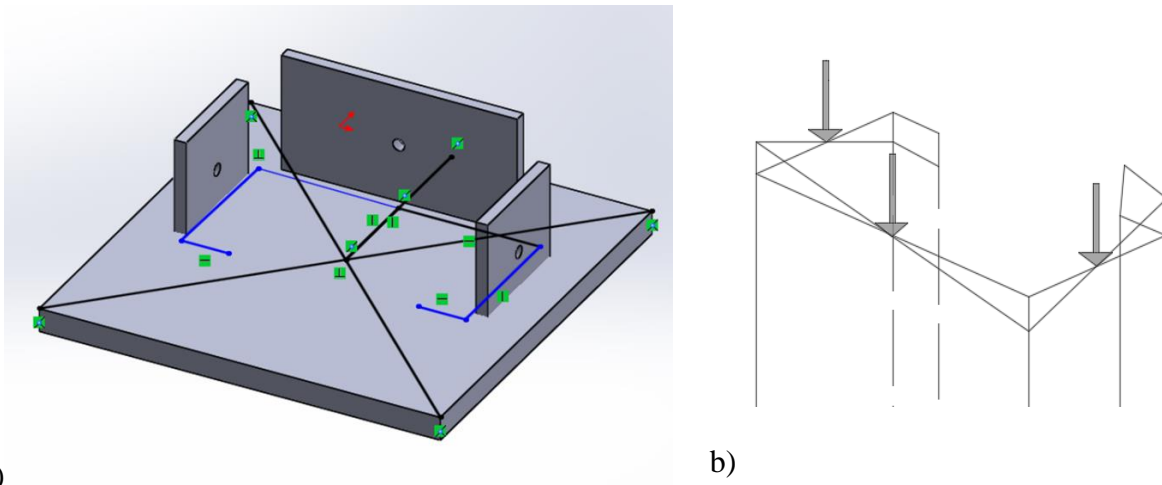
Figure 5: (a) End fixture to allow free warping (b) loading applied at zero sectoral co-ordinate

The specimens also have matching holes at the zero sectorial coordinate. The end fixture is bolted to the specimen with a gap to the end of plate as shown in Fig. 6 so that it allows free warping during loading. The load pass through bolts and not through the end plate. Since the specimen is made of thin plates and loads are applied through bolts, the specimen may undergo bearing failure. To avoid bearing failure of plate, small pieces of plate of 1.6 mm of thickness are welded around the bolted region. Thus, by increasing the thickness near the bolt region, bearing strength of specimen is increased. The effect of warping restrained due to increase in thickness will be very very less, since contour warping is predominant in case of lipped channel cross section when compared to thickness warping.

Figure 6: End condition to allow warping

3.4 Test setup and procedure

For warping restrained condition, the specimen is welded to end plate such that centroid of cross section and centroid of the plate are in same axis. A hardened plate is made with an indentation at center of gravity of plate and at points of desired application of load eccentricity. The advantages of this fixture are that the load can be applied eccentric to both the axes resulting in biaxial moment gradient along the length. To arrest torsional displacements, a small fixture is made such that it allows major axis bending and minor axis rotation while arresting the torsion. The specimen is carefully placed on the test setup on the spherical balls so that the required loading can be applied. The overall test setup and instrumentation adopted is shown in Fig. 7. The specimen is tested using the 500 KN MTS actuator with displacement control to capture the post bucking behaviour of the member. The experiments are conducted at a loading rate of 0.005 mm/sec.
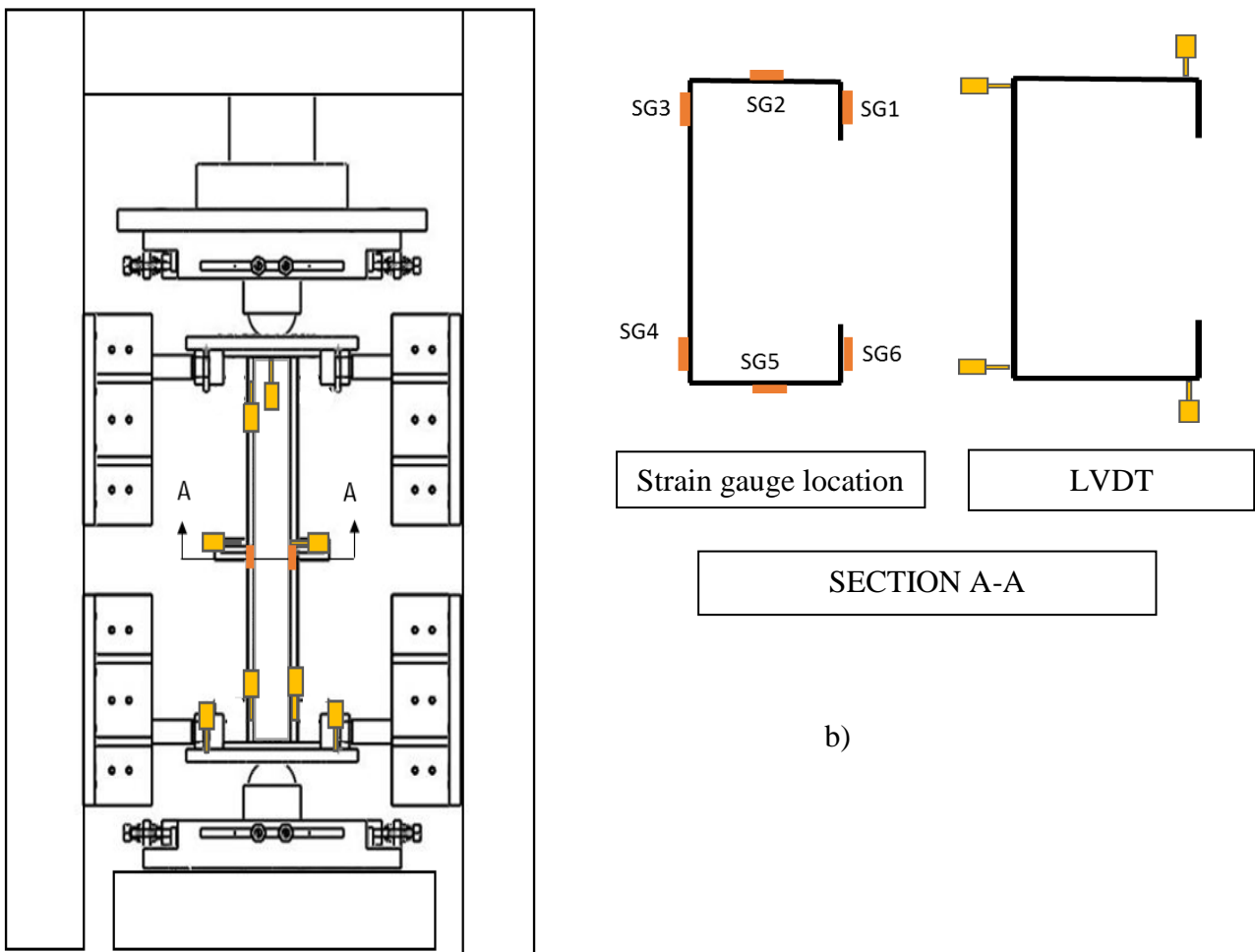
a)

Figure 7: a) Test setup b) Instrumentation scheme

Six strain gauges are used to measure the strain at the mid length of the member. 12 LVDTs are used, of which 4 LVDTs are placed at mid-length to measure the buckling deformation and twist of the cross section. 2 LVDTs are used at top and bottom end plates each to measure the rotation.

7

Another 4 LVDTs are used to measure the warping deformation in case of warping free boundary condition. The test specimens are labelled as shown in Fig. 8 based on the loading and boundary condition.
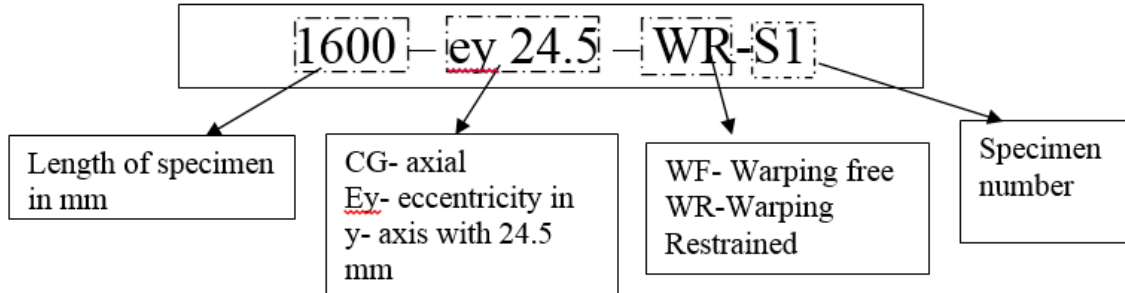
Figure 8: Nomenclature for the Test specimens

3.5 Test results

Totally sixteen tests are conducted with various loading and boundary condition. Each test is repeated twice to check the repeatability of the results. Members are tested for concentric and eccentric loading with warping free and warping restrained conditions. To understand the effect of warping on beam-column member, three tests are conducted where the eccentricities are varied along major axis. This study is limited to the members subjected to major axis bending with uniform moment at ends.

3.5.1 Axial load

The members are subjected to axial compression with both warping free and warping restrained boundary conditions. In case of axial compression, the member buckling is initiated in the flexural torsional buckling (FTB) mode. After large deflection and rotation, region at the center of member gets more stressed and fail due to distortional buckling and local buckling. Fig. 9 shows the buckling mode and load for the member under warping free and warping restrained condition. The torsional rotation of the cross section is significant, in case of warping free condition than warping restrained condition. Strain gauge results shown in Fig. 10 indicates that there is uniform strain along the cross-section during early part of the loading. Due to imperfection and twisting of cross section, the strain varies along the cross section with increase in load. There is strain reversal in some portion of cross section after peak because of FTB. Strain seen at the strain gauge location SG3 is due to local buckling at the mid-length of the specimen.

8
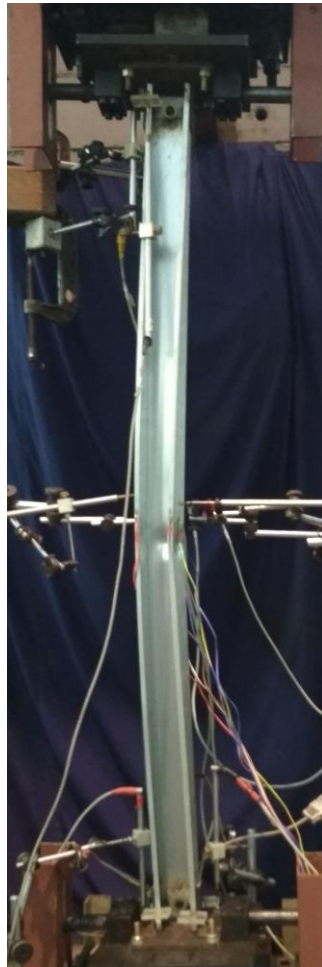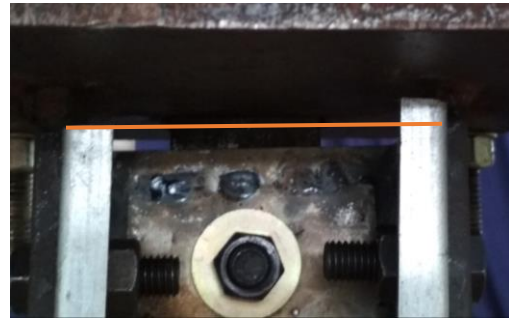
Warping deformation at top

Warping deformation at bottom

1600-CG-WR   1600-CG-WF

Figure 9: Failure buckling mode shape of under axial compression
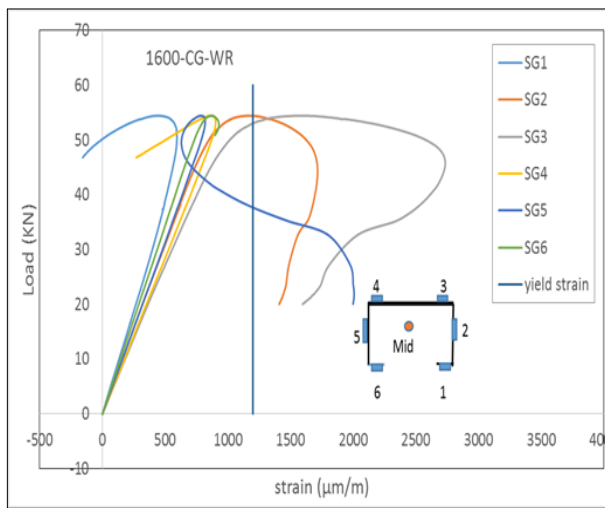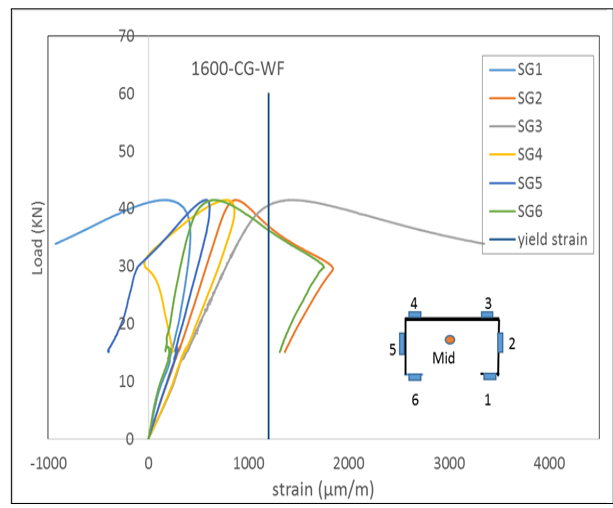
a)   b)

Figure 10: Axial load vs axial strain for members under axial compression a)warping Restrained b) warping Free

3.5.2 Beam-column behavior under eccentric compression

The effect of warping in case of beam-column is not documented much in the literature. Based on the theoretical buckling equation, members subjected to eccentric compression along major axis with warping free end condition, fails predominantly by FTB mode. The test results show similar behaviour of FTB in case of warping free condition. The member bends in major axis because of the eccentric loading along major axis. After reaching the critical load the member buckle with interaction of FTB and local buckling at the center of the member. This is clearly seen in all specimens with eccentric loading under warping free condition. A typical result is shown in Fig. 11.
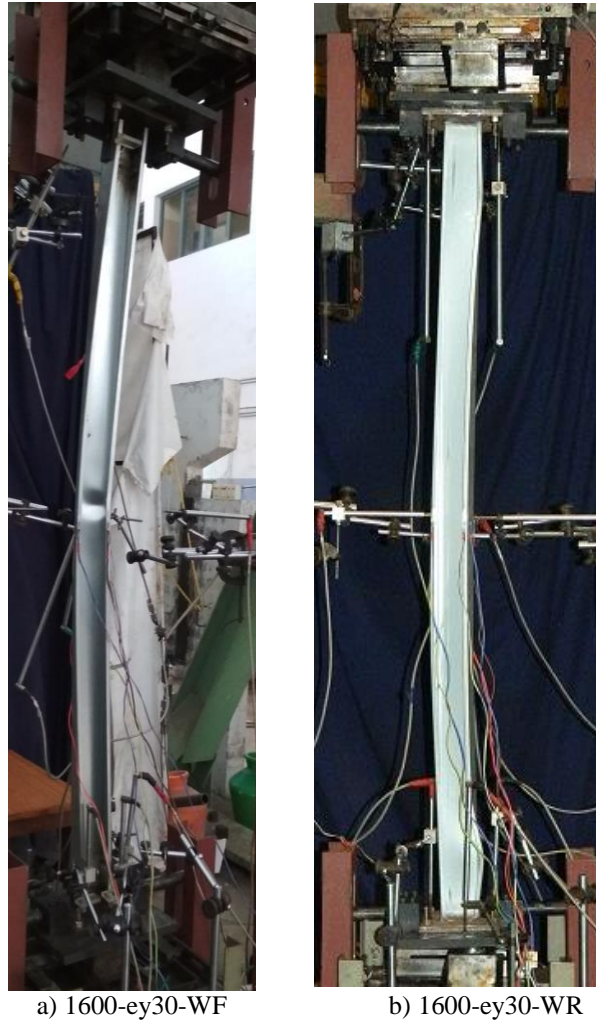
a) 1600-ey30-WF   b) 1600-ey30-WR
Figure 11: Typical failure mode for Beam column
a) warping free b) warping Restrained

In case of eccentric compression under warping restrained end condition, the member fails mainly due to interaction of global FTB and distortional buckling. Due to warping restraint, the global FTB buckling capacity increased which also trigger the initiation of distortional buckling mode. There is a clear change in buckling mode shape and failure load in case of warping restrained condition when compared to warping free condition. The summary of all the test results are given in Table 2. From the results we can infer that there was an increase in load

carrying capacity of around 30% in case of warping retrained condition compared to warping free end conditions.

Table 2: Test results with failure loads and modes

S. No.	Specimen	Load (Pmax) kN	Applied Moment kNmm	Average Load kN	Average moment kNmm	Failure Mode
1	1600-CG-WR-S1	54.43	0	53.71	0	FTB+D
2	1600-CG-WR-S2	53.00	0			FTB+L
3	1600-CG-WF-S1	41.53	0	41.01	0	FTB+D
4	1600-CG-WF-S2	40.5	0			FTB+L
5	1600-ey24.5-WR-S1	31.85	780.32	29.79	729.85	FTB+D
6	1600-ey24.5-WR-S2	27.73	679.38			FTB+D
7	1600-ey24.5-WF-S1	22.26	545.37	22.81	558.96	FTB+L
8	1600-ey24.5-WF-S2	23.37	572.56			FTB+L
9	1600-ey27-WF-S1	20.19	545.13	20.53	554.31	FTB+L
10	1600-ey27-WF-S2	20.87	563.49			FTB+L
11	1600-ey30-WR-S1	25.74	772.20	26.02	780.60	FTB+D
12	1600-ey30-WR-S2	26.3	789			FTB+D
13	1600-ey30-WF-S1	18.41	552.3	18.87	566.10	FTB+L
14	1600-ey30-WF-S2	19.33	579.9			FTB+L
15	1600-ey27-WR-S1	26.90	726.3	27.55	743.85	FTB+D
16	1600-ey27-WR-S2	28.20	761.4			FTB+D

4. Numerical study

The numerical modelling is conducted using finite element software ABAQUS 6.14. The elastic buckling analysis and nonlinear analysis of cold formed steel under axial load and beam column action is performed. The finite element model is validated with the test results. The finite element model is extended to other loading condition also. CFS members are modelled using shell S4R elements. Based on the mesh convergence study, 5×5 mm mesh size is adopted. The mechanical properties are taken from coupon test results.

4.1 Loading and support condition

In order to simulate the warping restrained condition and loading at CG point, multi point constraints (MPC) has been used as shown in Fig. 12. In case of warping free condition, the shell edge load is applied at the both the ends without restraining the displacement in axial direction. The model is restrained at the mid span to resist rigid body motion. Half-length model is used to reduce computational effort. In case of beam-column, shell edge load with varying compression is applied to simulate the stresses due to axial force and bending moment.

4.2 Analysis

The elastic buckling analysis gives the elastic critical load (P_{cr}), and buckling mode shape. While, the ultimate load is calculated using nonlinear analysis with static Riks solution procedure. The strength of CFS member is affected by the imperfections present in the members. Imperfection is applied as a combination of buckling modes as a result of buckling analysis with

standard scaling factors. The imperfection factors suggested by (Schafer and Peköz, 1998) for the various buckling (**L** = 0.34t and **D**= 0.54t, **G** = l/1000) is used in this study. The nonlinear analysis is carried out for all the test specimen in order to compare them with the experimental results.
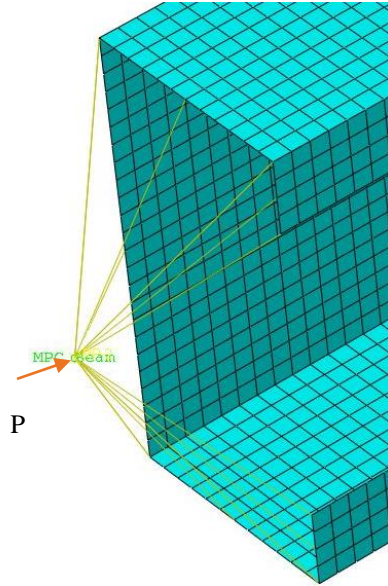
Figure 12: MPC constraints for warping
restrained case

4.3 Validation of numerical study with experiments
The results from the numerical study on beam-columns is compared with experimental results of the present study. Fig. 13a and 13b shows the failure mode due to axial load under warping restrained condition from experimental and numerical studies respectively. Ultimate loads compare very well with the experimental results. The failure is mainly due to interaction of distortional and global buckling. There is distortional buckling at top and bottom ends of the member with a combination of FTB and distortion at mid height. The failure mode predicted using numerical study shows a combination of global (FTB) distortional and local buckling at mid length of member in case of warping free boundary condition. The axial deflection and lateral deflection extracted from the numerical analysis are compared with the experimental deflection. The load deflection curve for axial compression is given in Fig. 14. The curve shows that the prediction of ultimate loads is good. The ultimate loads from the experiments and numerical investigations are compared in Table 3. The ultimate load for axial compression computed using the numerical model agrees very well with the results from experiments. A parametric study for prediction of ultimate strength is conducted by changing the eccentricity in the major axis direction. The numerical results are compared with beam-column design expressions prescribed in AISI S100-2016 using (i) LI framework and (ii) NLI framework using DSM.

12
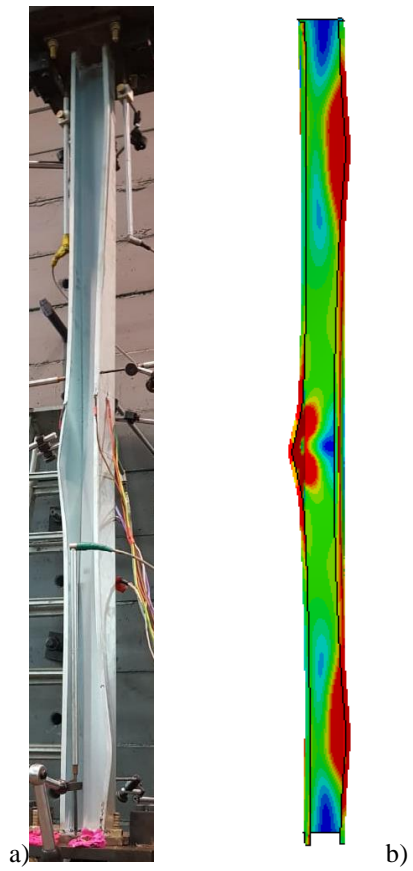
Figure 13: Failure mode a)experimental
b)Numerical result
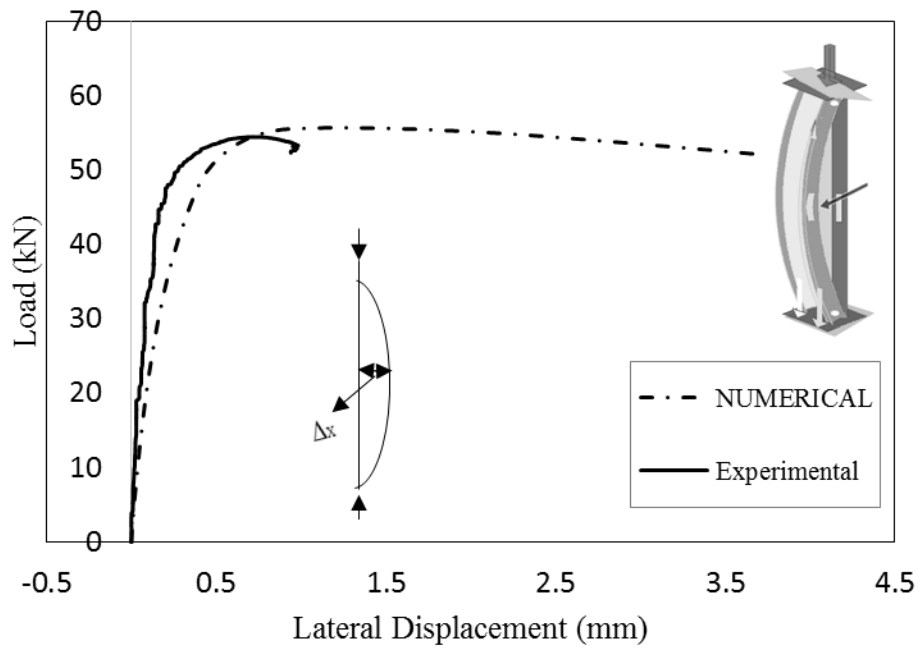
Figure 14: Validation of Numerical result with Experiment result

5. Discussion
5.1 Effect of warping and Bi-moment
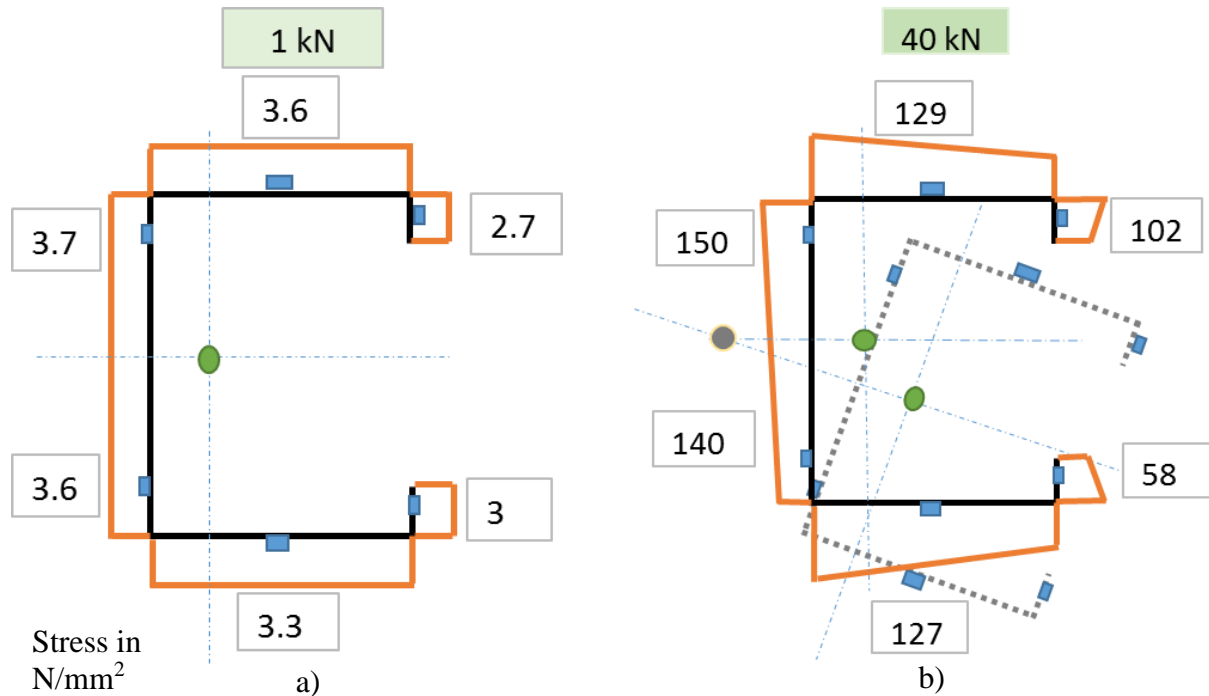
Figure 15: Stress distribution during axial compression loading a) 1kN b) 40 kN

The bi-moments are the secondary axial stresses which develop on the member due to the twisting deformation of the member. The twisting moment create a shear and axial stresses in the member. With respect to the cross section, this secondary axial stress will be self- equilibrating. Bi-moment can be represented as axial force multiplied by the sectorial coordinate at the point $(P \times \omega)$. The axial compressive stress on the cross section will not create an external bi-moment because they are self-equilibrating. But when a non-uniform stress due to bending and compression is applied on the cross section, there will be an additional external bi-moment. This bi-moment stresses along the cross section is not considered in case of generalized buckling formula developed for design using DSM. For this reason, the results of ultimate loads of the present experiments are conservative. Fig. 15 shows the plot of the actual stress calculated from strain gauge reading which shows the presence of bi-moment distribution. The stress, in cross section at loading of 1 kN shows the member is subjected to axial compression at very near to initial loading. The stress at a load 40 kN shows the combined stress due to axial force, bi-moment due to twist in the member and P- delta effect. Some strain gauges are placed at zero sectorial coordinate at flange, so that the strain gauge at the mid of the flange will capture stress without bi-moment. However, the strain gauges in web represents combination of these stresses.

It is seen from experiments that due to member twist with respect to shear center, the load eccentricity to the web of cross section decreases, and hence the compression stress in the web get increased than flanges. The stress gradient in the lip is due to the high variation of bi-moment stress in lip and due to change in eccentricity. The strain pattern obtained for warping free and warping restrained boundary condition follow similar pattern as the effect of bi-moment is

14

present in both the cases. The effect of bi-moment in the buckling strength will be generally neglected in the buckling formulation. However, the torsional behaviour is comprehended based on the shear flow. The additional axial force due to relative out of plane movement is generally neglected in design. Lip stiffeners play an important role in case of warping because of larger warping coordinates and deformability. To find the effect of warping on distortional buckling experiments results are needed on member which fail only due to distortional buckling on both warping free and warping restrained condition. Semi empirical Eq. (4) is found in the literature for the effect of warping restraint on distortional buckling. This formula is based on the numerical study on racks under distortional buckling is used in this study for warping effect on distortional buckling.

$$D_{boost} = 1 + 0.5\left(\frac{l}{lcrd}\right)^2 \tag{4}$$

5.2 Nonlinear Beam-Column Interaction framework

The nonlinear interaction (NLI) framework for design of beam-column is mainly based on the stability effects under actual combined stresses instead of considering individual stress action independently. In the NLI framework, the strength of member is represented by a single parameter β_n, instead of three components of applied stress in LI framework. The applied stress components are represented by β_r, θ_{mm} and ϕ_{pm} which is defined in Eq. (5), (6), and (7). The local buckling minima α_{crl} and distortional buckling minima α_{crd} from the signature curves for combined stresses have to be applied in equation (8).

$$\beta_r = \sqrt{x_r^2 + y_r^2 + z_r^2} \tag{5}$$

$$\text{where} \quad x_r = \frac{M_{r1}}{M_{y1}} \,, y_r = \frac{M_{r2}}{M_{y2}} \,, z_r = \frac{P_r}{P_y}$$

$$\theta_{mm} = tan^{-1}\left(\frac{y_r}{x_r}\right) \tag{6}$$

$$\phi_{pm} = cos^{-1}\left(\frac{z_r}{\beta_r}\right) \tag{7}$$

$$\beta_{cr} = \alpha_{cr}\,\beta_r, \, \beta_y = \alpha_y\,\beta_r \,, \, \alpha_y = \frac{F_y}{F_{max}} \tag{8}$$

Where M_{r1}, M_{r2} is a resultant applied moment in major axis and minor axis direction including P-δ and P-Δ effect and P_r is the applied axial load. DSM formula for beam and column is combined using Sine function as shown in Eq. (9). This NLI framework is developed based on the uniform stress throughout the member.

$$\beta_{nG} = \beta_{nGP} + \left(\beta_{nGM} - \beta_{nGP}\right)\,sin\phi_{PM} \tag{9}$$

The nonlinear interaction does not explicitly mention the moment gradient factor C_b and it conservatively assumes C_b as 1. In Finite strip method, the analysis can be performed only for the uniform stress throughout the member. Thus, C_m and C_b assumed as 1 may result inaccuracies in the calculation of member capacities. The C_b factor and C_m factor specified in the

design specification is developed based on the member subjected to moment alone. Thus, the effect of axial compression on the C_m and C_b factor is not considered. Since in NLI framework, the strength is based on resultant combined stress, applying same C_m and C_b factor needs further investigation. Thus, there is a need for the study in the area of defining the moment gradient factor in case of NLI framework. The implication and effect of moment gradient factor in NLI framework is studied in (Sevugan Rajkannu and Arul Jayachandran 2018). DSM based on CUFSM elastic buckling stress does not have a feature to consider the effect of warping on the buckling stress. The DSM prediction is mostly based on the signature curve which is developed based on the simply supported and warping free boundary condition. To include warping restrained effect the effective length factor K_t is used for torsional length. The use of CUTWP gives the elastic critical buckling load factor for global buckling based on the assumed effective length. Fig. 16 shows the comparison of test results for warping restrained for different values of K_t. The use of $K_t=0.5$ for warping restrained condition overestimate the capacity even in-case of axial compression. The use of $K_t=0.8$ gives reasonable prediction for the beam-column results although it is conservative in case of axial compression. Experiments on beam-columns also show that there is considerable effect on member capacities due to warping restraints. Fig. 17 shows the comparison of warping free test results with LI and NLI. There is a marked difference between the experimental result and numerical results in case of beam-columns which may be due to the different loading condition. Numerical results are closer to the member resistance expressions using NLI framework. NLI framework equation is mainly developed based on the numerical result and validated it with few experimental results with members failed by flexural buckling. To incorporate the effect of warping on beam-column member design, more experiments are needed, mainly on members prone to fail in FTB mode. For predicting the beam-column strength for warping restrained condition a simple procedure using GBTUL buckling strength is developed in this study. Since GBTUL has a capability of finding buckling strength for various boundary condition, the buckling results from GBTUL are applied in the NLI framework equation and final predictions are tabulated in Table 3. There appears to be a discrepancy in using CUTWP for beam-column design for global buckling. The global buckling result from the CUFSM and CUTWP vary even in case of warping free condition. Thus, using CUTWP for global buckling in case of warping restrained condition in NLI needs further investigation.

Table 3: Comparison of Test result with linear interaction LI and NLI

| S.No | specimen name | Experiment | | | | Numerical | |
		P_{Test} kN	LI for $K_t=0.7$	LI for $K_t=0.5$	NLI GBTUL	$P_{numerical}$ kN	$P_{numerical}/$ P_{test}
1	1600-CG-WR	53.72	1.06	0.88	1.05	53.05	1.01
2	1600-ey24.5-WR	29.79	0.97	0.88	1.04	33.63	0.89
3	1600-ey27-WR	27.55	0.91	0.82	1.01	32.28	0.85
4	1600-ey30-WR	26.02	0.92	0.84	1.02	30.81	0.84
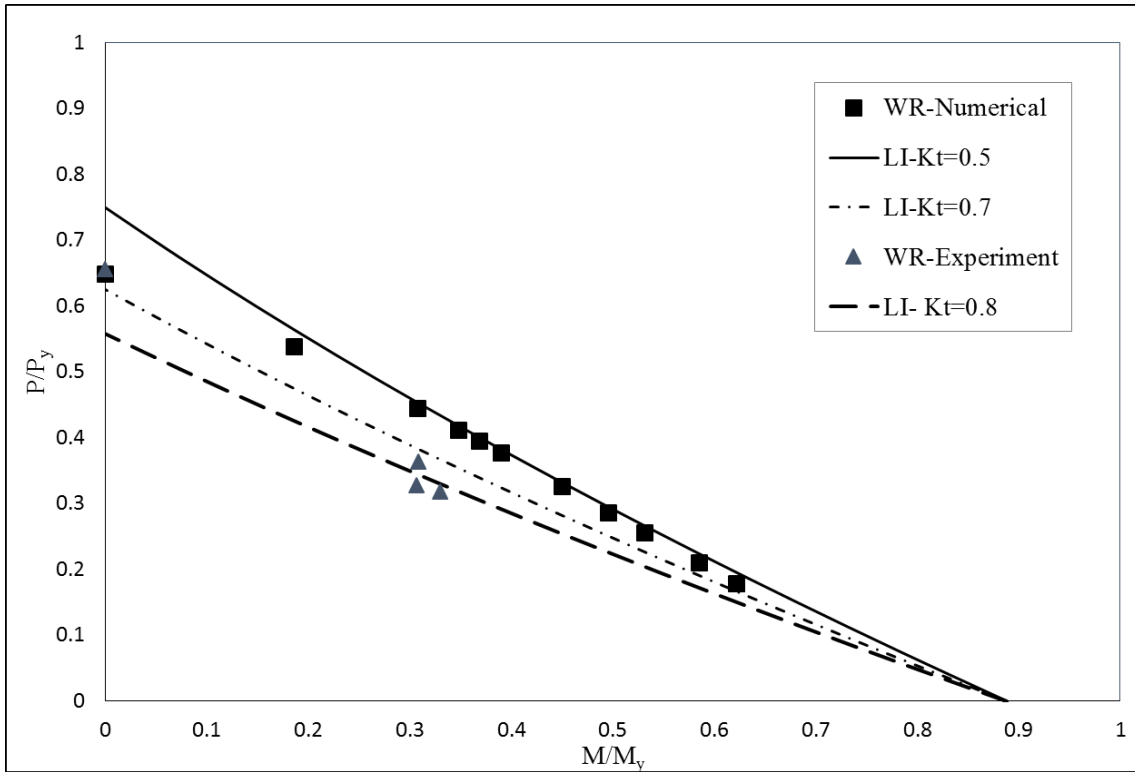
Figure 16: Comparison of P-M capacities with LI for warping restrained boundary condition
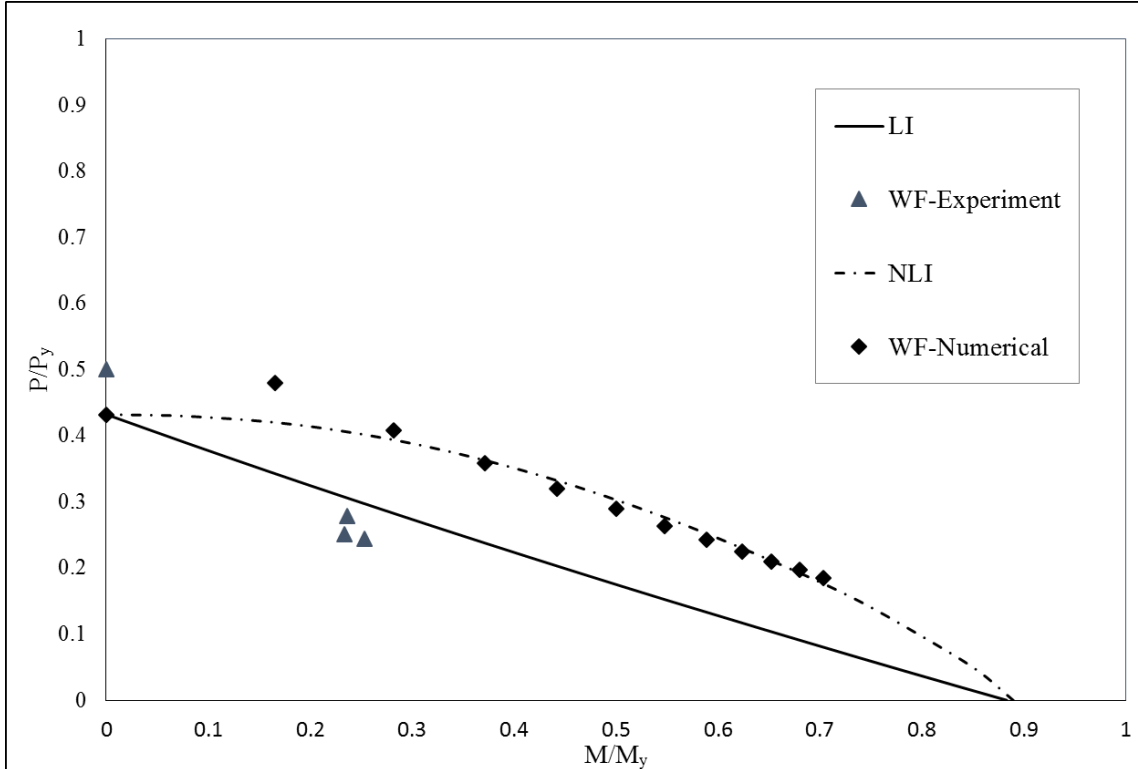
Figure 17: Comparison of P-M capacities with LI and NLI for warping free boundary condition

6. Summary and conclusions

The primary intent of this paper is to critically examine the implementation of stability design of CFS beam-columns by focusing on the aspect of warping. Carefully conducted experimental and numerical investigations reported in this paper are the primary basis on which the following conclusions are drawn. It is pointed that the present code provisions (AISI S100-16) pertaining to design of CFS members, especially in beam- columns, have no clear guidance on accounting for warping as a design parameter. Experiments on beam-columns show that warping induces qualitative and quantitative differences in behaviour when one chooses to allow it or restrain it. It has been shown in this paper that the effects of warping cannot be neglected as insignificant. In the qualitative aspect, the present experiments brought out a fact that for a given cross section and length, the CFS members fail predominantly by flexural torsional buckling in case of warping free end condition and by interaction of distortional and flexural torsional buckling in case of warping restrained end condition.

When the beam –column capacities of CFS members are calculated using the classical linear interaction framework (AISI S100-16) using DSM, it is observed that the use of effective length factor for warping restraint K_t=0.5 lead to overestimation of the capacity in-case of axial compression. With the present experimental results, it is seen that the use of warping restraint factor K_t=0.8 results in acceptably close predictions of beam-column capacities using the LI framework.

The authors computed capacities using DSM LI and NLI for beam-columns by computing the global buckling capacity using the software CUTWP. However, the aspect of warping handled through the torsional effective length is a still a grey area and authors could not get consistent results for the beam column capacities.

From the present study it has been observed that numerically simulated implementation of warping in the NLI framework is much deviated from the results of the present experimental investigation. Hence the authors are in the process of generating experimental data pool to further validate the NLI framework.

7. References

AISI-S100. (2016). "North American Specification for the Design of Cold-Formed Steel Structural Members". Washington (DC, USA): *American Iron and Steel Institute*

Ádány S., Schafer, B. W. (2006). "Buckling mode decomposition of single-branched open cross-section members via finite strip method: Application and examples". *Thin-Walled Structures*, *44*(5), 585–600.

Bian, G., Peterman, K. D., Torabian, S., Schafer, B. W. (2016). "Torsion of cold-formed steel lipped channels dominated by warping response". *Thin-Walled Structures*, *98*, 565–577.

Camotim, D., Basaglia, C., Silvestre, N. (2010). "GBT buckling analysis of thin-walled steel frames: A state-of-the-art report". *Thin-Walled Structures*, *48*(10–11), 726–743.

Chen, W.F., Atsuta, T. (1976). "*Theory of Beam Columns*". McGraw-Hill International Book Company, New York.

Gunalan, S., Mahendran, M. (2013). "Improved design rules for fixed ended cold-formed steel columns subject to flexural-torsional buckling". *Thin-Walled Structures*, *73*, 1–17.

Huang, Y., Young, B. (2014). "The art of coupon tests". *Journal of Constructional Steel Research*, *96*, 159–175.

Kalyanaraman, V., Jayabalan, P. (1994). "Local buckling of stiffened and unstiffened elements under nonuniform compression". *International Specialty Conference on Cold-Formed Steel Structures: Recent Research and Developments in Cold-Formed Steel Design and Construction*, 1–9.

Kalyanaraman, V., Rao, K. S. (1998). "Torsional-flexural buckling of singly symmetric cold-formed steel beam columns". *Journal of Constructional Steel Research*, *46*(1–3), 191–193.

Kumar, M. V. A., Kalyanaraman, V. (2014). "Distortional buckling of CFS stiffened lipped channel compression members". *Journal of Structural Engineering (United States)*, *140*(12), 1–14.

Li, Y. L., Li, Y. Q., Song, Y. Y., Shen, Z. Y. (2016). "In-plane behavior of cold-formed thin-walled beam-columns with lipped channel section". *Thin-Walled Structures*, *105*, 1–15.

Miller, T. H., Pekoz, T. (1994). "Load-eccentricity effects on cold-formed steel lipped-channel columns". *Journal of Structural Engineering New York, N.Y.*, *120*(3), 805–823.

Moore, D. B., Currie, D. M. (1988). "Warping Restraint, Member Stability and Standards". *9th International Specialty Conference on Cold-Formed Steel Structures*, 97–113.

Pekoz, T., Winter, G. (1969). "Torsional-flexural buckling of thin walled sections under eccentric load". *Journal of Structural Engineering*, *ASCE 95*(4), 941–963.

Piana, G., Lofrano, E., Manuello, A., Ruta, G., Carpinteri, A. (2017). "Compressive buckling for symmetric TWB with non-zero warping stiffness". *Engineering Structures*, *135*, 246–258.

Prokić, A., Mandić, R., Vojnić-Purčar, M., Folić, R. (2015). "Torsional buckling of thin-walled beams in presence of bi-moment induced by axial loads" *Technicki vjesnik* 22, 1, 183-189.

Rasmussen, K.J.R. (2006). "Design of slender angle section beam-columns by the Direct Strength Method", (February), 204–211.

Rhodes, J., Macdonald, M., McNiff, W. (2000). "Buckling of cold formed stainless steel columns under concentric and eccentric loading". *International Specialty Conference on Cold-Formed Steel Structures: Recent Research and Developments in Cold-Formed Steel Design and Construction*, 687–699.

Schafer, B.W. (2012). "Development of DSM Direct Design Formulas for Beam-Columns" Year 1 Report, John Hopkins University, Baltimore.

Schafer, B. W. (2008). "Review: The Direct Strength Method of cold-formed steel member design". *Journal of Constructional Steel Research*, *64*(7–8), 766–778.

Schafer, B. W., Peköz, T. (1998). "Computational modeling of cold-formed steel: characterizing geometric imperfections and residual stresses". *Journal of Constructional Steel Research*, *47*(3), 193–210.

Sevugan Rajkannu, J., Arul Jayachandran, S. (2018). "Investigations on the design implementation of cold- formed steel beam-column members using direct strength method", *Proceedings of the eighth thin walled steel structure conference.* Lisbon (1), 1–10.

Torabian, S., Fratamico, D. C., Schafer, B. W. (2015). "Experiments on cold-formed steel Zee-shaped stub beam-columns". *Structural Stability Research Council Annual Stability Conference 2015, SSRC 2015*, 1–18.

Torabian, S., Zheng, B., Schafer, B. W. (2014). "Experimental study and modeling of cold-formed steel lipped channel stub beam-columns". In *Structural Stability Research Council Annual Stability Conference 2014, SSRC 2014* (pp. 380–401).

Vijayavengadesh Kumar, J., Arul Jayachandran, S. (2016). "Experimental investigation and evaluation of Direct Strength Method on beam-column behavior of uprights". *Thin-Walled Structures*, *102*, 165–179.

Vlasov, V. Z. (1961). "Thin-Walled Elastic Beams". Israel Program for Scientific Translations.